KOMPSAT-2 AOCS Control Mode & Power Safe Mode Design

Seung-Wu Rhee*, Hak-Jung Kim and Joo-Jin Lee*****
KOMPSAT Program Division, Korea Aerospace Research Institute, Taejon, 305-333, Korea

Abstract

KOMPSAT-2 is the second Korean earth observation satellite after KOMPSAT-1: the 1 meter GSD cartographic capability and planning to launch at the end of 2005 by ROKOT launch vehicle. The dedicated AOCS operational modes are designed for KOMPSAT-2 based on KOMPSAT-1 experience All of AOCS operational modes requires gyro information. To compensate this drawback, Power Safe Mode is designed and implemented. Successfully AOCS on-board software is developed and extensively verified through a nonlinear simulation process. The simulation results of Power Safe Mode and Science Fine Submode are provided to demonstrate its functionality as well as its performance.

Key Word : KOMPSAT-2, spacecraft, attitude & orbit control system, control mode, power safe mode, B-dot

Introduction

KOMPSAT-2 is the second Korean earth observation satellite after KOMPSAT-1 launched successfully in December 1999. KOMPSAT-2 is a high resolution Low Earth Orbit(LEO) satellite that is under developing in Korea for the 1 meter panchromatic and 4 meter multi-spectral image data collection. It is planning to launch at the end of 2005 by ROKOT launch vehicle and place in a 685 km sun synchronous orbit(inclination angle is 98.13deg. and mean local time of ascending node is 10:50AM).This type of high resolution imaging mission flows down stringent requirements to the spacecraft Attitude & Orbit Control System in terms of pointing accuracy, pointing knowledge, rate stability, etc.

The purpose of this paper is to provide an overview of the AOCS design results including the key features of AOCS from the requirement point of view, AOCS operation concept and its design results.

The structural system of KOMPSAT-2 has hexagonal configuration to maximize internal space. The length of its deployed configuration is about 6.8m and its height is 2.5m. Total mass is about 800kg and the required power is about 1.1kW. The deployed configuration is shown in Figure 1.

KOMPSAT-2 basically consists of three modules: payload module, avionic module, and propulsion module. The payload module is designed to minimize thermal distortion and to securely accommodate a high resolution camera. And the camera electronic components such as payload management unit, data compression & storage unit, and some of AOCS sensors are located in this module. Most of AOCS components such as reaction wheel assembly, gyro unit, star tracker and

* AOCS Department Head
** Satellite Division Director
*** KOMPSAT Program Manager
E-mail : srhee@kari.re.kr, TEL : 042-860-2447, FAX : 042-860-2603

associated electronics are mounted in the avionics module.

KOMPSAT-2 is a 3-axis stabilized spacecraft using zero momentum bias method to provide flexibility in operation and expandability in future program. The attitude information is measured by two star trackers, or earth sensors and sun sensors depending on a selected operational control mode. Four reaction wheels or four hydrazine thrusters are used to control the spacecraft attitudeas well as to maintain an orbit the pointing accuracy is less than 0.025degree (3 sigma steady state in roll and pitch axes), the pointing knowledge is less than 0.02degree, the position knowledge is provided by a GPS receiver. Solar Array Drive Assembly that is a kind of stepping motor, is rotating to face the solar array toward the Sun when spacecraft is nadir-pointing. AOCS hardware connection configuration is depicted in Figure 2.

The high resolution camera provides 1 meter panchromatic and 4 meter multi-spectral imagery simultaneously. Its image swath is 15km. The detector system employs the pushbroom imaging technique; the TDI(Time Delay Integration) concept is utilized for PAN imaginary to increase SNR(TDI level of maximum 32)

AOCS Overview

The Attitude & Orbit Control System of KOMPSAT-2 is developed based on the highly reliable KOMPSAT-1 spacecraft launched with the 6.6 meter panchromatic camera successfully in the end of 1999 and still now normally operating. Main differences between KOMPSAT-1 and KOMPSAT-2 can be stated as follows:

KOMPSAT-2 is employing a strap-down star tracker and gyros to provide stringent pointing accuracy while KOMPSAT-1 using an earth sensor and gyros. From the operational concept point of view, a wheel-based back-up recovery concept is introduced to enhance its operational robustness in addition to KOMPSAT-1 design concept whose recovery concept from contingency was designed based on thruster-based control. As a normal operational concept, gyro sets are autonomously configured by on-board software after spacecraft is separated from launch vehicle. Autonomous gyro selection logic is newly developed for the dedicated KOMPSAT-2 gyro: Northrop Grumman's SIRU whose mechanical and operational concept is totally different from KOMPSAT-1 gyro, Kearfott's TARA gyro. Also, PIID controller along with Star Tracker based Kalman filter scheme instead of PI controller used in KOMPSAT-1, is developed and adapted to meet the stringent pointing requirements.

As shown in figure 1, 4 coarse sun sensors are mounted at the corners of solar array to cover 4 Pi field of view.

As shown in figure 2, RDU that is a dedicated AOCS on-board Intel processor x386 with math-coprocessor, two star trackers, two earth sensors, three-axis magnetometer, one gyro unit, three magnetic torque rods are interconnected for AOCS functioning properly.

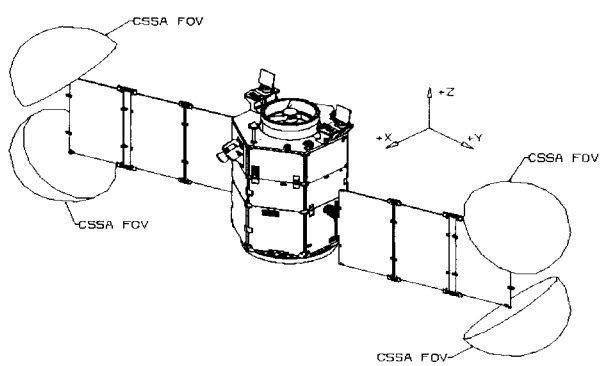

Fig. 1. KOMPSAT-2 Deployed Configuration

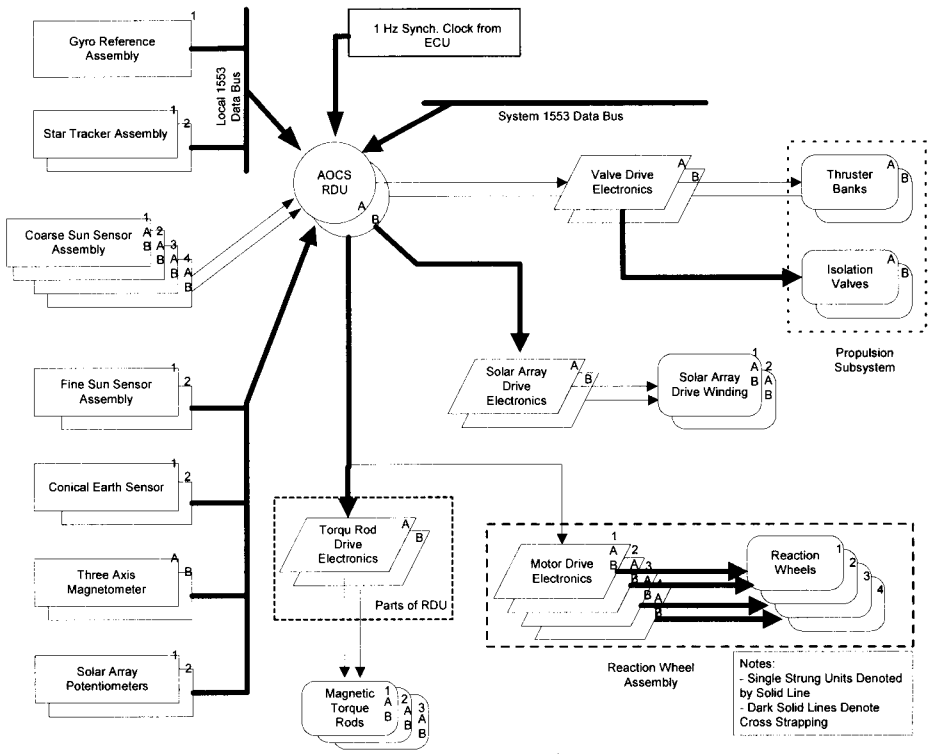

Fig. 2. AOCS Hardware Connection Diagram

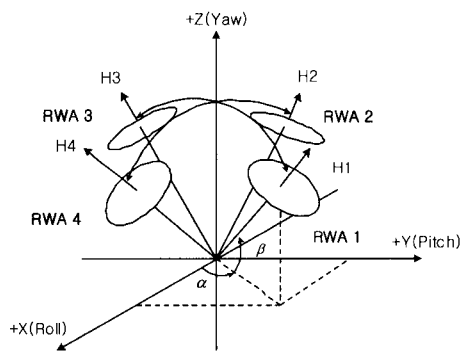

Fig. 3. Pyramid Type of Reaction Wheel Configuration

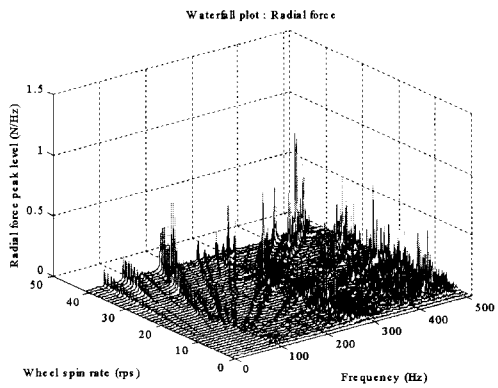

Fig. 4. Waterfall Plot of Radial Force of RWA

Figure 3 shows the installed configuration of 4 reaction wheels arranged in pyramid configuration of $4/\sqrt{3}\,(1\times 1\times 1)\,h$ about the spacecraft yaw axis to provide an equal angular momentum capability to each axis.

For taking the high resolution camera image, the LOS jitter and rate stability are one of the critical factors to be considered in design phase. In KOMPSAT-2 system, 4 reaction wheels are main source to introduce LOS jitter to the high resolution camera. Thus, micro-vibration measurement test of RWAs was extensively performed to identifythe micro-vibration level that influences to the system level jitter. Figure 4 shows the waterfall plot of radial directional forceof RWA with respect to the wheel speed as well as frequency ranges.

Design Results

AOCS Control Mode Design[1]

The AOCS utilizes five distinct control modes that consist of eleven separate and distinct control submodes; six submodes of them are taken from KOMPSAT-1 heritage and the rest of five submodes are newly developed to provide more operational flexibility as well as robustness to KOMPSAT-2.

Sun Mode

Sun Mode consists of three submodes(Sun Pointing Submode, Earth Search Submode, Safe Hold Submode) that perform different tasks while the spacecraft body is inertially fixed and the arrays are sun-pointing. In all submodes of Sun Mode, the coarse sun sensors and the gyros are the only control sensors and the thrusters are the only control actuators.

Sun Point Submode

This submode providesthe capability to point the solar array normal to the sun starting from an arbitrary initial attitude in sunlight. During eclipse transitions, all axes are held fixed inertially with integrated gyro information. This submode isused for attitude stabilization following solar array deployment after launcher separation.

Earth Search Submode

When Earth Search Submode is enabled by the ground command, the AOCS begins a roll maneuver at a specified rate and automatically transition the spacecraft from Sun Point Submode (two-axis attitude control) to Attitude Hold Submode (nadir pointing attitude, three-axis LVLH control) based on information from the Conical Earth Sensors.

Safe Hold Submode

Safe Hold Submode isfunctionally equivalent to Sun Point with two exceptions: the gains and deadbands are changed to maximize fuel savings and all redundant equipment (with the exception of gyros) is used in the control loop. The solar arrays are driven to the initial deployed position.

Maneuver Mode

Maneuver mode consists of two submodes(Attitude Hold Submode, Del-V Submode) that perform different functions while the spacecraft is either inertially fixed or pointed relative to a LVLH reference. In all submodes of Maneuver Mode, the gyros and Conical Earth Sensors as well as Fine Sun Sensors are the control sensors depending on a selected submode, and the thrusters are the only control actuators.

Attitude Hold Submode

This submode provides the capability for three-axis attitude control relative to either an inertial or LVLH reference. Two distinct functions are performed: attitude hold with respect to either reference or attitude maneuvers relative to either reference. When nadir-pointed, the LVLH reference is updated using Conical Earth Sensor(CES) and Fine Sun Sensor(FSS) data. This submode supports entry into Science Mode.

Del-V Submode

This submode providesthe capability for three-axis attitude control relative to an inertial or LVLH reference while nominally firing all four thrusters. Attitude control is accomplished by off-modulating the thrusters to counter external disturbance torque.

Science Mode

Science mode consists of two submodes(Science Coarse Submode, Science Fine Submode) that perform similar functions with different sensors for attitude updates while the spacecraft is pointed relative to a LVLH reference. In all submodes of Science Mode, the gyros are used for attitude propagation.

Science Coarse & Fine Submode

The Science Coarse Submode and the Science Fine Submode are functionally identical except that the Science Coarse Submode uses CESs and FSSs while the Science Fine Submode uses Star Trackers for attitude updates: The Science Coarse Submode provides Zero Momentum Bias (ZMB) 3-axis stabilized attitude control using Gyros, CESs, FSSs and RWAs. The nominal attitude in this mode is LVLH reference. Attitude control errors are generated by subtracting the estimated attitude, derived from the propagated gyro reference with updates from CESs and FSSs, from the command attitude derived from On-Board Ephemeris Propagator with GPS data or On-Board Ephemeris Propagator with an uploaded ephemeris data. The roll, pitch and yaw attitudes are actively controlled by reaction wheel torques. Nominally, allfour wheels have a bias speed that prevents attitude transients caused by passing through zero wheel speed. In the event of wheel failure, reaction wheels are run about zero nominal bias speed with special software compensation to reduce the effect of transitioning through zero wheel speed.

Back-up Mode

The main difference of Back-up Mode and Sun Mode is that Back-up Mode utilizes reaction wheel assembly instead of thruster banks to save its propellant. Back-up Mode consists of three submodes(Back-up Sun Pointing Submode, Back-up Earth Search Submode, Back-up Attitude Hold Submode) : two submodes that perform different tasks while the spacecraft body is inertially fixed and the arrays are sun-pointing, and one submode that provides the capability for three-axis attitude control relative to LVLH frame. In all submodes of Back-up Mode, the gyros are used for attitude control.

Back-up Sun Pointing Submode

The Coarse Sun Sensors(CSS) and the gyros are the only control sensors and the reaction wheels are the control actuators. The magnetic torquers are activated for the momentum unloading purpose.

This submode provides the capability to point the solar array normal to the sun starting from an arbitrary initial attitude in sunlight. During eclipse transitions, all axes areheld fixed inertially with integrated gyro information. This submode will be used for attitude stabilization by ground command only.

Back-up Earth Search Submode

The CSSs and the gyros are the only control sensors and the reaction wheels are the control actuators. The magnetic torquers are activated for the momentum unloading purpose.

When Back-up Earth Search Submode is enabled by the groundcommand, the AOCS beginsa roll maneuver at a specified rate and automatically transition the spacecraft from Back-up Sun Point Submode (two-axis attitude control) to Back-up Attitude Hold Submode (nadir pointing attitude, three-axis LVLH control) based on information from the CESs.

Back-up Attitude Hold Submode

The CESs and the gyros are the only control sensors and the reaction wheels are the control actuators. The magnetic torquers are activated for the momentum unloading purpose. No filter estimation is required.

This submode provides the capability for three-axis attitude control relative to LVLH reference using the reaction wheels as the actuator. When nadir-pointed, the roll and pitch axes will be controlled using CES and the yaw axis using the gyro compassing from gyro data. This submode supports entry into Science mode by ground command.

Power Safe Mode

The Tri-Axis Magnetometer(TAM) and the CSSs are the only control sensors and the magnetic torquers are the control actuators. No gyro data is required. This mode is used for attitude stabilization in case that the automated gyro selection logic fails or gyro is malfunctioning during the period of spacecraft deployment as well as normal operational period. Also, once Power Control Unit memory relay associated with Power Safe Mode activation is enabled by ground

command, spacecraft will mode-transition to this mode instead of Safe Hold Submode whenever malfunction occurs.

This mode provides the capability to damp out the initial rate of spacecraft and to align the roll axis of spacecraft with the sun vector with the constant roll rate starting from an arbitrary initial attitude in sunlight. During eclipse transitions, the pitch and yaw axes are held fixed inertially with the constant roll rate.

AOCS Control Mode Transition

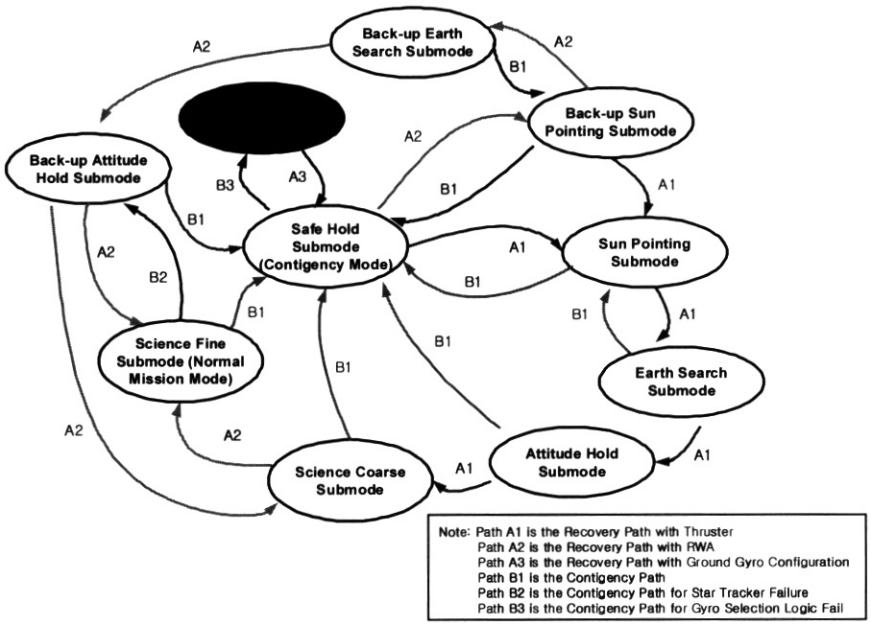

Fig. 5. AOCS Control Mode Transition Diagram

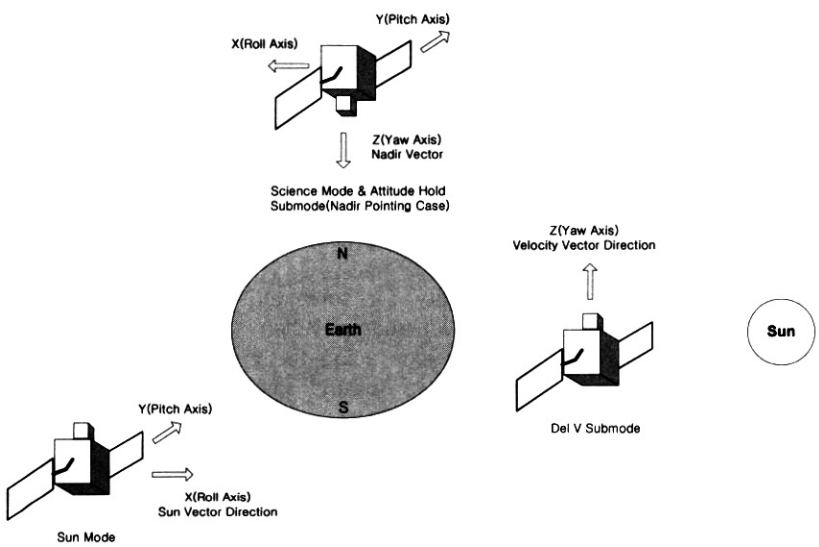

Fig. 6. Spacecraft Attitude of Each Submode

Figure 5 describes the AOCS control mode transition flow. A2, A3, B2 and B3 paths in figure are newly developed to increase an operational flexibility and robustness for KOMPSAT-2. Note that all the modes except Power Safe Mode requires the spacecraft rate information from gyro. As depicted in figure 6, spacecraft is nadir-pointing in Science Mode and Attitude Hold Submode and Back-up Attitude Hold Submode, and the solar array is pointing to the sun in Sun Mode, Back-up Sun Pointing Submode and Power Safe Mode.

The detail formulation and design results of Power Safe Mode will be introduced in the next section.

Power Safe Mode[1,2]

Power Safe Mode consists of two control schemes: B-dot control law to reduce an initial rate or tip-off rate, and simple spinning stabilization controller to provide an angular momentum and to secure sun in case that gyro unit is malfunctioning or is not properly configured.

B-dot Control

Following simple B-dot control law is utilized to damp-out the initial rate of spacecraft at the first stage of the Power Safe Mode.

$$\vec{M} = -K \cdot \dot{\vec{B}}_{body} \tag{1}$$

,where $\vec{M}$, $\dot{\vec{B}}_{body} = \dot{\vec{B}}_{ECI} - \vec{w} \times \vec{B}_{body}$ are magnetic dipole moment by magnetic torque rod and the magnetic field change rate in body frame respectively, and $\dot{\vec{B}}_{ECI}$ is the field change in ECI frame.

Its global stability is well known in many public domains as: Assuming the kinetic energy equation as a Lyapunov function

$$T = \frac{1}{2} \vec{w}^T I \vec{w} > 0 \tag{2}$$

The time derivative of the kinetic energy is

$$\dot{T} = \dot{\vec{w}}^T I \vec{w} = \vec{\tau} \cdot \vec{w} \tag{3}$$

,where external torque $\vec{\tau} = I\dot{\vec{w}}$ if $\vec{H} = I\vec{w}$.

The control torque acting on the spacecraft due to B-dot control law is

$$\vec{\tau} = \vec{M} \times \vec{B}_{body} \tag{4}$$

Substituting Eq. (4) into Eq. (3) gives Eq. (5).

$$\dot{T} = (\vec{M} \times \vec{B}_{body}) \cdot \vec{w} = (\vec{B}_{body} \times \vec{w}) \cdot \vec{M} \tag{5}$$

Using B-dot control law Eq. (1), Eq. (5) can be expressed in

$$\dot{T} = K \dot{\vec{B}}_{ECI} \cdot \vec{B}_{body} - K \vec{B}_{body} \cdot \vec{B}_{body} \cong -K \vec{B}_{body} \cdot \vec{B}_{body} < 0 \tag{6}$$

,where generally $\vec{B}_{body} \gg \dot{\vec{B}}_{ECI}$

Thus, as shown in Eq. (6), B-dot control law globally stabilizes the system.

Simple Spinning Stabilization Controller[2]

The simple spinning stabilization with this controller is basically equivalent to the major axis spinning method that is dynamically robust and stable: if the body spins about any axis except the major axis and there exists some internal energy dissipation due to a fuel sloshing or vibration of flexible appendage, spinning axis will eventually transfer to the major axis in order to

satisfy the below equation.

$$T_{\min} = \frac{1}{2}\frac{h^2}{I_{\max}} \tag{7}$$

When the spacecraft is rotating at the rate of Ω about the x-axis(major axis) of spacecraft pointing toward the sun, the sun vector can be decomposed into three axis components of spacecraft frame. Also, if the x-axis of spacecraft is pointing to the sun and the $y$and z components of sun vector in body frame are small enough to neglect, the sun vector in body frame can be expressed in following form without loss of generality:

$$\vec{S}_B = \begin{Bmatrix} \sqrt{(1-y^2-z^2)} \\ y \\ z \end{Bmatrix} \cong \begin{Bmatrix} 1 \\ y \\ z \end{Bmatrix} \tag{8}$$

Suppose $\Omega >> \omega_x$, then the spacecraft body rate in body frame is approximated as

$$\vec{w}_B \cong \begin{Bmatrix} \Omega \\ w_y \\ w_z \end{Bmatrix} \tag{9}$$

Let the sun vector in the inertia frame define as $\vec{S}_I = [\ X\ \ Y\ \ Z\ ]^T$. Suppose the sun vector is constant in certain time period without loss of generality, the time derivative of sun vector is as follows:

$$\begin{aligned} \dot{\vec{S}}_I &= \dot{\vec{S}}_B + \vec{w}_B \times \vec{S}_B \\ \vec{0} &\cong \begin{Bmatrix} 0 \\ \dot{y} \\ \dot{z} \end{Bmatrix} + \begin{Bmatrix} w_y z - w_z y \\ w_z - z\Omega \\ y\Omega - w_y \end{Bmatrix} \end{aligned} \tag{10}$$

Thus, the relationship between the sun vector change rate $\dot{y}$, $\dot{z}$ and body rate w_y, w_z is obtained as following:

$$\begin{aligned} w_y &= \dot{z} + y\Omega \\ w_z &= -\dot{y} + z\Omega \end{aligned} \tag{11}$$

Total angular momentum of the spinning spacecraft with the rate of Ω about the x-axis is

$$\vec{H} = \begin{Bmatrix} I_x(w_x+\Omega) \\ I_y w_y \\ I_z w_z \end{Bmatrix} \tag{12}$$

And the time derivative of the total angular momentum in ECI is written in

$$\left.\frac{d\vec{H}}{dt}\right|_I = \left.\frac{d\vec{H}}{dt}\right|_B + \vec{w} \times \vec{H} = T_c \tag{13}$$

,where T_c is external torque: control torque or disturbance torque,

and $\vec{w} \times \vec{H} = \begin{Bmatrix} (I_z - I_y) w_y w_z \\ (I_x - I_z) w_z (w_x + \Omega) \\ (I_y - I_x) w_y (w_x + \Omega) \end{Bmatrix}$ is called as a gyroscopic coupling term.

Neglecting higher order term, Eq. (13)can be simplified as

$$I_x \dot{w}_x = T_{xc} \tag{14a}$$

$$I_y \dot{w}_y + (I_x - I_z)\Omega w_z = T_{yc}$$

$$I_z\dot{w}_z+(I_y-I_x)\Omega w_y=T_{zc} \tag{14b}$$

,where I_x, I_y, I_z are the moment of inertia of spacecraft, T_{xc}, T_{yc}, T_{zc} are control torque for each axis.

For the x-axis rate control that provides robustness of stability with respect to an external disturbance by providing angular momentum to the x-axis of spacecraft, a simple rate control scheme can be introduced as following:

$$T_x=-k_s w_x \tag{15}$$

To secure the sun ray on the face of solar array, simple PD controller is used in y- and z-axis control respectively. The y and z components of sun vector in body frame from sun sensors as well as rate information from three axis magnetometer(TAM) are fed back to control the spacecraft attitude as following:

$$\begin{aligned} T_y&=-k_n w_y+k_p y \\ T_z&=-k_n w_z+k_p z \end{aligned} \tag{16}$$

Now, to design a controller and to demonstrate its stability, we can use Eq. (11) that shows the relationship between rates and the sun vector change of y and z component in body frame.

And the derivatives of Eq. (11) are

$$\begin{aligned} \dot{w}_y&=\ddot{z}+\dot{y}\Omega \\ \dot{w}_z&=-\ddot{y}+\dot{z}\Omega \end{aligned} \tag{17}$$

Using above relationship, the closed-loop systems of y and z axis in body frame are expressed as follows:

$$\begin{aligned} &\ddot{y}+\frac{k_n}{I_z}\dot{y}+\alpha\,\Omega^2 y+\{\alpha-1\}\Omega\,\dot{z}+\frac{1}{I_z}(k_p-k_n\Omega)z=0 \\ &\ddot{z}+\frac{k_n}{I_y}\dot{z}+\beta\,\Omega^2 z-\{\beta-1\}\Omega\,\dot{y}-\frac{1}{I_y}(k_p-k_n\Omega)y=0 \end{aligned} \tag{18}$$

,where $\alpha=\dfrac{(I_x-I_y)}{I_z}>0$, $\beta=\dfrac{(I_x-I_z)}{I_y}>0$

If we take it Laplace Transform, the results are

$$\begin{bmatrix} s^2+\dfrac{k_n}{I_z}s+\alpha\Omega^2 & \{\alpha-1\}\Omega s+\dfrac{1}{I_z}(k_p-k_n\Omega) \\ -\{\beta-1\}\Omega s-\dfrac{1}{I_y}(k_p-k_n\Omega) & s^2+\dfrac{k_n}{I_y}s+\beta\,\Omega^2 \end{bmatrix}\begin{Bmatrix} y \\ z \end{Bmatrix}=\begin{Bmatrix} 0 \\ 0 \end{Bmatrix} \tag{19}$$

The characteristic equation of Eq. (19) is

$$\begin{aligned} &s^4+k_n\left(\frac{1}{I_y}+\frac{1}{I_z}\right)s^3+\left[\Omega^2(\alpha+\beta)+\frac{k_n^2}{I_yI_z}+(\alpha-1)(\beta-1)\Omega^2\right]s^2+ \\ &\left[k_n\Omega^2\left(\frac{\alpha}{I_y}+\frac{\beta}{I_z}\right)+\Omega(k_p-k_n\Omega)\left\{\frac{(\alpha-1)}{I_y}+\frac{(\beta-1)}{I_z}\right\}\right]s+\alpha\beta\,\Omega^4+\frac{1}{I_yI_z}(k_p-k_n\Omega)^2=0 \end{aligned} \tag{20}$$

The necessary condition of stability is that all of coefficients are positive. To make it satisfy the necessary condition, the simplest choice is $k_p-k_n\Omega=0$ which defines the relations of proportional gain k_p, rate gain k_n and the predefined x-axis spin rate Ω. The selected condition makes $\Omega(k_p-k_n\Omega)\left\{\dfrac{(\alpha-1)}{I_y}+\dfrac{(\beta-1)}{I_z}\right\}=0$, which is a part of coefficients of s and part of

constant term. Thus, the final characteristic equation becomes

$$s^4 + k_n\left(\frac{1}{I_y}+\frac{1}{I_z}\right)s^3 + \left[\Omega^2(\alpha+\beta) + \frac{k_n^2}{I_yI_z} + (\alpha-1)(\beta-1)\Omega^2\right]s^2 + k_n\Omega^2\left(\frac{\alpha}{I_y}+\frac{\beta}{I_z}\right)s + \alpha\beta\ \Omega^4 = 0 \tag{21}$$

As seen in Eq. (21), all coefficients of polynomial are positive with the positive rate gain, k_n if the predefined x-axis spin rate $\Omega > 0$.

It is known that the structured singular value,μ, accurately predicts system robust stability characteristics. To check the stability robustness, μ analysis is performed and figure shows the structured singular value plot. From the μ plot in figure, the peak lower bound μ value is about 1. Thus, the H_∞ norm of the smallest destabilizing perturbation is about 1.0

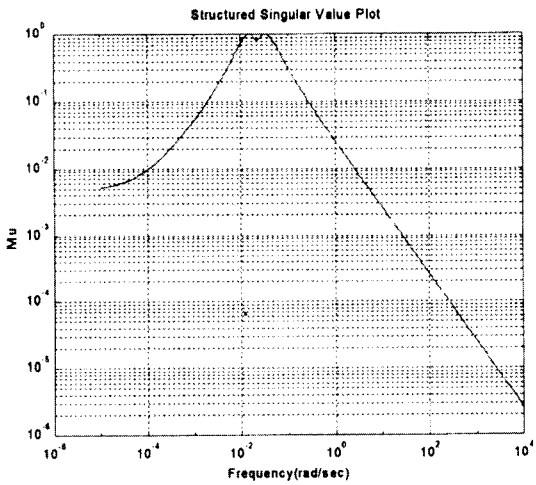

Fig. 7. Structured Singular Value Plot

Simulation Results

The nonlinear simulation is extensively performed to verify the performance and to validate the functionality of AOCS. The detailed models of actuators as well as sensors are used in

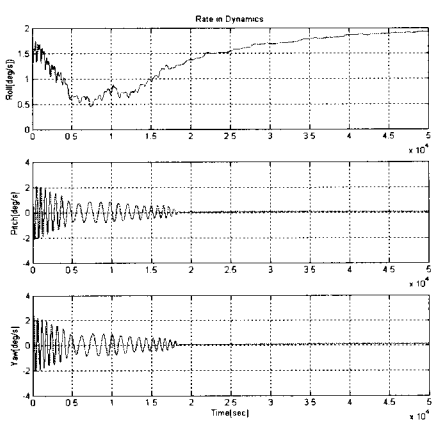

Fig. 8. Body Rate Plot of Power Safe Mode

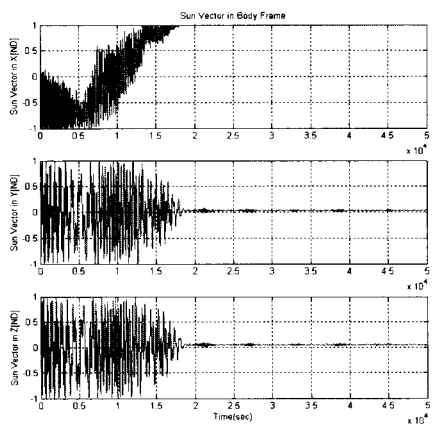

Fig. 9. Sun Vector in Body Frame

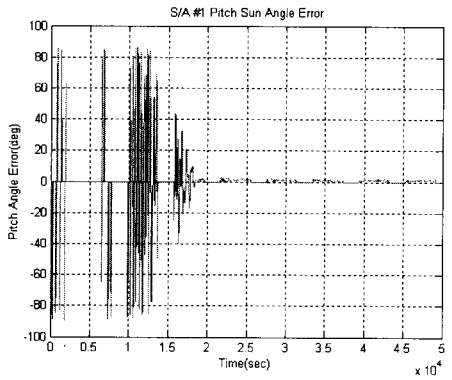

Fig. 10. Sun Angle Error in Pitch Axis

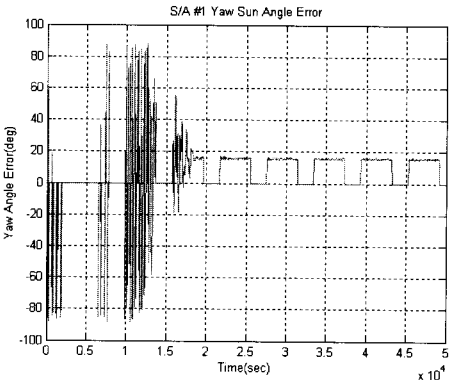

Fig. 11. Sun Angle Error in Yaw Axis

simulation. Further more, the flight software that is identical to the on-board software is used for simulation to represent a real situation. Figures 8 to 11 show the performance of Power Safe Mode. Spacecraft rate profile is plotted in figure 8 starting from an initial condition of 2.0 deg/sec per each axis. As seen in figure, B-dot controller is at the beginning activated to damp-out the body rate to almost 0.5 deg/sec. As shown in figure 9, the sun vector is aligned to the x-axis of spacecraft at the steady sate from arbitrary initial condition after about 3 orbits(18000 seconds). The pointing accuracy requirement of pitch and yaw axes is 20 degree. Figure 10, 11 show the pointing accuracies of pitch and yaw axes in the solar array frame; the solar array is pointing to the sun properly. KOMPSAT-2 solar array is canted by 17.5 degree due to 10:50am MLTAN. The constant yaw angle error in figure 11 shows the solar array canted angle of 17.5 degree that is steady state error. Figures 12 and 13 demonstrate the performances of Science Fine Submode: LOS rate stability of 0.0015 deg/sec, pointing accuracy of 0.025 deg. for roll and pitch axes, and 0.04deg. for yaw axis.

Conclusions

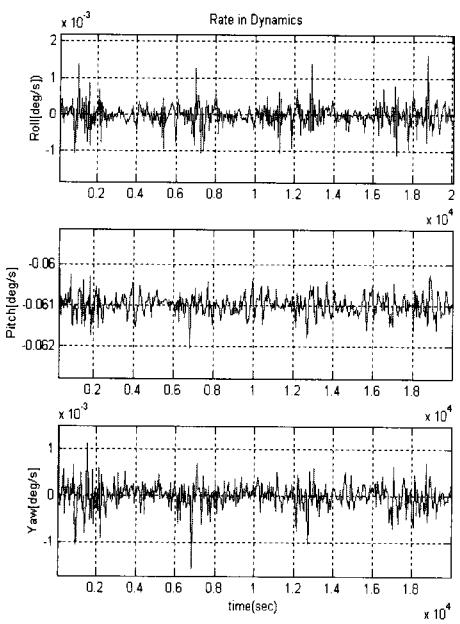

Fig. 12. Body Rate in Science Fine Submode

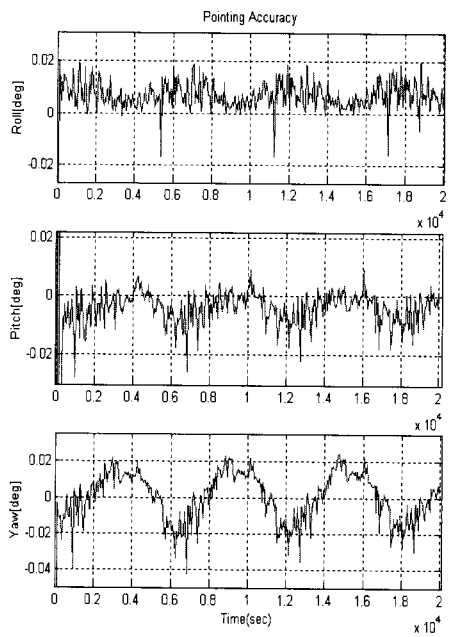

Fig. 13. Pointing Accuracy in Science Fine Submode

AOCS operational concept of KOMPSAT-2 as well as the control logics is successfully developed and implemented to meet the 1 meter high resolution imaging mission requirements. The control algorithm of Power Safe Mode without gyro information is implemented to provide an operational flexibility and to overcome possible malfunction of gyro unit as well as autonomous gyro selection logic. To avoid a burring effect on cartographic image, the pointing stability as well as the micro-vibration effects is considered at AOCS design phase through an extensive test and analysis. As a result of micro-vibration test with RWAs that are main vibration sources, it concludes that system satisfies the jitter requirements. The nonlinear KOMPSAT-2 AOCS simulator imbedded an on-board flight software, is developed to validate the operation sequences of AOCS and to verify the performance of control logics required for successful KOMPSAT-2 mission in Korea. Simulation results show that the LOS rate stability, pointing accuracy and pointing knowledge requirements are satisfied.

Acknowledgement

The authors wish to acknowledge that this work was financially supported by the Ministry of Science & Technology and the Ministry of Commerce, Industry & Energy, Korea.

References

1. S.-W. Rhee, 2002, KOMPSAT-2 Subsystem Specification for the Attitude & Orbit Control Subsystem(KARI Internal Doc.).

2. MTI & ASE, 2002, KOMPSAT-2 Magnetic Sun Pointing Safehold Interim Report.